



Segmentation on remote sensing imagery for atmospheric air pollution using divergent differential evolution algorithm

Meera Ramadas¹ · Ajith Abraham¹

Received: 24 February 2022 / Accepted: 3 October 2022
© Springer-Verlag London Ltd., part of Springer Nature 2022

Abstract

Air pollution is a global issue causing major health hazards. By proper monitoring of air quality, actions can be taken to control air pollution. Satellite remote sensing is an effective way to monitor global atmosphere. Various sensors and instruments fitted to satellites and airplanes are used to obtain the radar images. These images are quite complex with various wavelength differentiated by very close color differences. Clustering of such images based on its wavelengths can provide the much-needed relief in better understanding of these complex images. Such task related to image segmentation is a universal optimization issue that can be resolved with evolutionary techniques. Differential Evolution (DE) is a fairly fast and operative parallel search algorithm. Though classical DE algorithm is popular, there is a need for varying the mutation strategy for enhancing the performance for varied applications. Several alternatives of classical DE are considered by altering the trial vector and control parameter. In this work, a new alteration of DE technique labeled as DiDE (Divergent Differential Evolution Algorithm) is anticipated. The outcomes of this algorithm were tested and verified with the traditional DE techniques using fifteen benchmark functions. The new variant DiDE exhibited much superior outcomes compared to traditional approaches. The novel approach was then applied on remote sensing imagery collected from TEMIS, a web based service for atmospheric satellite images and the image was segmented. Fuzzy Tsallis entropy method of multi-level thresholding technique is applied over DiDE to develop image segmentation. The outcomes obtained were related with the segmented results using traditional DE and the outcome attained was found to be improved profoundly. Experimental results illustrate that by acquainting DiDE in multilevel thresholding, the computational delay was greatly condensed and the image quality was significantly improved.

Keywords TEMIS · OMI · Air quality · Mutation · Entropy · Thresholding

1 Introduction

Air pollution forms one of the biggest threats to the existence of the living organisms in our earth. It is a mix of gas with solid particles suspended in air released by car exhaust, exhaust from industries, dust, etc. The variations in ozone, water vapor, methane, nitrous oxide, and carbon dioxide all lead to changes in climate and air quality. Acidic depositions, ozone hole depletion, greenhouse gas effect is some of the changes observed in nature due to

pollution. Understanding the concentration and severity of any such pollutant that exist in atmosphere and its effect on nature, human or on the society is a challenge for scientist and researcher working in the field of remote sensing.

Environmental monitoring comprises of monitoring and characterizing the features and composition in our environment, which in our case is to explicitly monitor the air quality. Remote sensing deals with gathering of data about any phenomenon or object without coming in to any kind of physical contact with them. The remote sensing instruments are two types, namely active and passive. In case of active instruments, they deliver the source of energy to the monitored object or scene and then capture the radiation. On the other hand, passive instruments capture natural energy, which is being emitted or reflected from the monitored object or scene. Sunlight reflected from the

✉ Meera Ramadas
mramadas@ucb.edu.bh

¹ Machine Intelligence Research Labs (MIR Labs), Scientific Network for Innovation and Research Excellence, Auburn, WA 98071, USA

object is a natural source of radiation that is received by the passive instrument sensor. These sensors, when used in atmospheric remote sensing, will be tuned precisely to the required wavelengths.

Numerous satellites installed with specialized remote sensing instruments have been launched till date to measure air quality. SCIAMACHY (SCanning Imaging Absorption spectroMeter for Atmospheric CartographY) is a submissive spectrometer for observing transmitted, emitted or scattered radiations from earth's surface and atmosphere. It measures the wavelength range between 240 and 2380 nm. This instrument is placed in ENVI-SAT satellite. SCIAMACHY takes the measurement of global traces of aerosols and atmospheric gasses suspended in stratosphere and troposphere. The instrument consists of a telescope, a spectrometer, a mirror system, and thermal and electronic sub systems. The Ozone Monitoring Instrument (OMI) is used for pollution climate studies. It measures backscattered and reflected light in visible and ultraviolet parts of spectrum. OMI measures the amount of UV rays and gasses like nitrogen dioxide, sulfur dioxide, etc. reaching the ground from high above the surface and helps forecasters to give warning to public. GOME used for monitoring atmospheric Ozone across the global is a nadir scanning ultraviolet and visible spectrometer.

The TEMIS (Tropospheric Emission Spectrometer) program purpose is to capture, compute and publish results on global concentration of traces of various gas in troposphere captured from nadir-viewing satellite instruments like OMI (Ozone Monitoring Instrument), SCIAMACHY and GOME. The European Space Agency (ESA) run Data User Program (DUP) champion the TEMIS project. Measurement of Pollution In The Troposphere (MOPITT) is the gadget aboard the NASA EOS-Terra satellite, measuring the global concentration of carbon monoxide (CO) in troposphere.

The volume of data that can be collected from such remote sensing instruments are huge and it needs extraordinary computational backing. The analyzed data output from the remote sensing instruments are generally false color images that distinguish even the slightest of difference within the radiation wavelength in reference to the environment composition that is being analyzed. Therefore, there is a need for segmenting the image into various wavelengths to study the level of pollution in a particular area in detail and to deliver public alerts accordingly. Thresholding is an elementary method of image segmentation in which the imagery is converted to

foreground and background pictures. Colored imageries employ the color components on the basis of color spaces for thresholding. Issues such as thresholding are categorized as unsupervised learning and these can be cracked with evolutionary approaches.

Evolutionary technique employees the biotic procedures of reproduction, recombination, selection and mutation. Storn and Price [1] announced the DE technique that uses the thoughts of evolutionary practices. DE is a population-based approach which aids in unraveling optimization topics effectually. DE algorithm determines its efficiency and performance through control parameter and the trial vectors generation approach. Though DE algorithm is widely used owing to its advantages, its performance is affected by the choice of control parameters. Several alternatives of classical DE are considered by altering the trial vector and control parameter.

In this research, a modification of DE termed Divergent Differential Evolution strategy (DiDE) was created where four dissimilar mutation scale factors are employed. By employing four control parameters, the performance of the new variant is enhanced in comparison to the performance of classical DE approach. This approach is correlated with the additional standard variations through tables to authorize improved competence of DiDE. This approach is applied in image thresholding for segregating the atmospheric remote sensing imagery based on definite wavelengths. Multilevel image thresholding uses the concept of fuzzy Tsallis entropy together with the altered DE method to achieve image segmentation. The initial segment of the work describes technique for thresholding and fuzzy Tsallis entropy method of thresholding. The following segment elaborates the DE method and the anticipated variant that was created. The remaining sections describe the application of the new approach in multilevel thresholding and the outcomes that were gained following the work.

2 Related works

Image segmentation is an optimisation problem that uses evolutionary concepts for its implementation. A number of variants of DE has been developed through research and these variants have been applied for numerous areas of image processing. Few of the works related to variants and their application in image processing are listed out in tabular form below.

Author	Application in image segmentation	Author	Application in image segmentation
Tang et al. [2]	A study to execute machine vision on the basis of weed detection technology for open-air natural illumination situations was performed. A binary-coded genetic algorithm (GA) was used for supervised color image segmentation in his color space. On comparison with other segmentation results from cluster analysis, this technique achieved better performance	Ghamisi et al. [15]	They presented two methods of segmenting an image using Darwinian PSO and Fractional order Darwinian PSO. Effectiveness of the techniques were related and verified
Tsai et al. [3]	The challenges in image segmentations and image smoothing using the concept of Mumford Shah paradigm from the perspective of curve evolution are addressed in this work	Sarkar and Das [16]	They proposed a multilevel threshold on the basis of 2D histogram for improving the segmentation of object pixels. The multilevel thresholding was performed using maximum Tsallis entropy. The projected method was verified on standard datasets
Jiang and Yang [4]	They developed an evolutionary Tabu search technique for image segmentation. The projected technique was found to be efficient for solving global optimisation problems	Bhandari et al. [17]	They implemented a variant of Cuckoo search and wind driven optimisation technique for thresholding images by means of Kapur's entropy. Outcomes obtained were compared and efficiency was justified
Tao et al. [5]	A three-level thresholding technique for image breakdown was projected on the basis of entropy theory, fuzzy partition and probability partition. The consequences obtained demonstrated that the proposed technique gave improved performance	Sağ and Çunkaş [18]	They developed a colour segmentation technique based on a new optimisation technique named as improved bee colony multi-objective optimisation (IBMO). The technique was applied on several images from Berkley database
Ramos and Fernando [6]	They used unsupervised k-means technique in Genetic algorithm. This technique was tested on color maps, human skin mark segmentation, etc.	Ramadas et al. [19]	They developed a variation of DE named Reconstructed Differential Evolution (ReDE). This variant was tested with traditional mutation strategies and ReDE showed improved results in evaluation to other strategies
Omran et al. [7]	They developed an image clustering technique using particle swarm optimization	Meng and Pan [20]	This work proposed a novel parameter-reduced differential evolution methodology. This approach removed the crossover rate parameter Cr by using an spontaneously produced crossover matrix and gives a self-adaptive tuning order of F value
Das et al. [8]	They developed PSO based segmentation technique to automatically group pixels of the image in to diverse regions. In this technique, spatial information of images is introduced into membership function for clustering	Suresh and Shyam [21]	They proposed modified DE algorithm for enhancing the brightness and contrast of satellite images
Omran et al. [9]	They developed Dynamic Clustering Approach (DCPSO) on the basis of particle swarm optimisation. This technique finds the optimal count of clusters automatically, clustering the dataset using limited user interference. This technique was tested on complex images and their results proved its efficiency	Meng et al. [22]	They proposed PaDE algorithm which has superior performance in comparison to other state-of-the-art DE variants
Talbi et al. [10]	They proposed a split/merge technique using the results from k-means algorithm as the input for quantum evolutionary algorithm	Meng and Pan [23]	They proposed a new categorized archive-based trial vector generation strategy with depth information of evolution. It provided a improved opinion of settings of objective functions and also improved the candidate diversity of the trial vectors
Maitra and Chatterjee [11]	They gave an improved hybrid of PSO algorithm. This technique employed histogram-based image segmentation for multi-level thresholding	Ramadas et al. [24]	They projected another modification of DE algorithm termed as FSDE. This approach was used for data clustering and the efficiency of the approach was verified
Maulik [12]	A comprehensive assessment on medical image segmentation was given by implementing genetic algorithm	Ramadas and Ajith [25]	They introduced another hybrid of DE named Transformed Differential Evolution which showed heightened results for detecting tumors in MRI images
Das and Sil [13]	They devised an improved DE algorithm to cluster an image using gray scale space. This method does not need to know the number of clusters initially	Krishna and Ravi [26]	They implemented binary differential evolution for customer segmentation
Ma et al. [14]	They devised a method for segmenting Synthetic Aperture Radar (SAR) images using Artificial Bee Colony (ABC) Algorithm. Here, ABC is used for finding the ideal threshold value. This technique was compared with other evolutionary techniques		

Author	Application in image segmentation
Singh and Bose [27, 28]	They initially introduced a novel optimisation algorithm FFQOA with k means clustering for segmentation of chest CT images of COVID-19 patients. In the second work, they also formulated a new image clustering algorithm based on ambiguous set theory
Singh [29]	T2NS based image segmentation algorithm for segmenting MRIs of brain tumor was proposed in this work

3 Background study

3.1 Differential evolution

In an n-dimensional search space, the nominated amount of vectors are identified informally. In each reiteration, more than one vectors are selected indiscriminately within the populace and are combined to formulate a novel vector. The resulting vector is related to pre-agreed target vector to generate a trial vector. If trial vector offers an apt objective function, then the trial vector is recognized to subsequent group. Mutation, recombination and selection are performed until certain terminating norm is accomplished. DE utilize the population of NP candidate solutions indicated by $X_{i,G}$, in which index $i = 1, 2, \dots, NP$ establish populace while G represent the group of populace.

3.1.1 Mutation

Mutation makes DE exceptional in contrast to additional evolutionary practices. The weighted difference of vectors in the group is calculated. For any specified variable $X_{i,G}$, take three vectors $X_{r1,G}, X_{r2,G}$ and $X_{r3,G}$ indiscriminately where r_1, r_2, r_3 are varied from one another. Donor vector $V_{i,G}$ is calculated below:

$$V_{i,G} = X_{r1,G} + F \times (X_{r2,G} - X_{r3,G}) \tag{1}$$

The mutation factor F is a persistent within (0,2). The given strategy is symbolized as DE/rand/1. The mutation equation discriminates one DE technique from the other. The utmost repeatedly used DE codes are:

$$\text{DE/rand/2} \quad V_{i,G} = X_{r1,G} + F \cdot (X_{r2,G} - X_{r3,G}) + F \cdot (X_{r4,G} - X_{r5,G}) \tag{2}$$

$$\text{DE/best/1} \quad V_{i,G} = X_{best,G} + F \cdot (X_{r1,G} - X_{r2,G}) \tag{3}$$

$$\text{DE/best/2} \quad V_{i,G} = X_{best,G} + F \cdot (X_{r1,G} - X_{r2,G}) + F \cdot (X_{r3,G} - X_{r4,G}) \tag{4}$$

$$\text{DE/rand-to-best/1} \quad V_{i,G} = X_{r1,G} + F \cdot (X_{best,G} - X_{r2,G}) + F \cdot (X_{r3,G} - X_{r4,G}) \tag{5}$$

3.1.2 Crossover/recombination

This operation uses prosperous solutions in the populace. Trial vector $U_{i,G}$ is produced for target vector $X_{i,G}$ using binomial crossover. Using probability $C_r \in [0, 1]$, the members of donor vector go into trial vector. Crossover probability C_r is designated together with populace size NP .

$$U_{j,i,G+1} = \begin{cases} V_{j,i,G+1} & \text{if } \text{rand}_{ij}[0, 1] \leq C_r \text{ or if } j = I_{\text{rand}} \\ X_{j,i,G+1} & \text{if } \text{rand}_{ij}[0, 1] > C_r \text{ or if } j \neq I_{\text{rand}} \end{cases} \tag{6}$$

$\text{rand}_{ij} \approx \cup[0, 1]$ and I_{rand} is a random numeral from $1, 2, \dots, N$.

3.1.3 Selection

Trial vector and vector in current population determines the final population for next generation. Target vector $X_{i,G}$ is tied to trial vector $V_{i,G}$ and bottommost result of function is engaged in succeeding generation.

$$X_{i,G+1} = \begin{cases} U_{i,G+1} & \text{iff } (U_{i,G+1}) \leq f(X_{i,G}) \text{ where } i = 1, 2, \dots, N \\ X_{i,G} & \text{otherwise} \end{cases} \tag{7}$$

3.2 Divergent mutation strategy

In DiDE, we have used four control parameters. The constraint F identified as amplifying parameter takes a constant value among (0,2) and F1 takes the complement of constraint F. The new parameter N1 takes a fluctuating value amid (0,1) and N2 takes the complement of N1. As four dissimilar control parameters are chosen, the donor vectors are boosted significantly and hence the efficacy of DiDE approach is improved intensely. The use of four control parameters increases the mutation probability. The CPU time taken will decrease with higher mutation probability. By considering best solution vector, this style overlaps quicker in comparison to the conventional strategies having arbitrary vectors alone. The variables $X_{r1,G}, X_{r2,G}, X_{r3,G}, X_{r4,G}, X_{r5,G}$ are chosen arbitrary. The proposed strategy is given as:

$$X' = X_{r1,G} + F \cdot (X_{r2,G} - X_{r3,G}) - F1 \cdot (N1 \cdot (X_{best,G} - X_{r4,G}) - N2 \cdot (X_{best,G} - X_{r5,G})) \tag{8}$$

By using four varied control constraints, the resultant donor vector has been intensified and hence the effectiveness of DiDE algorithm is also intensified immensely. By

Table 1 Comparative results for different strategies of DE with DiDE

Function	D	DE approaches					DiDE	Significance
		DE/best/1	DE/rand/1	DE/best-to-rand/1	De/best/2	DE/rand/2		
Sphere	50	9.743e−016	6.95e−016	7.514e−016	9.67e−016	7.175e+0	7.013e−016	−
	25	9.345e−015	9.36e−015	9.529e−015	9.44e−015	6.923e+000	8.85e−015	+
Schwefel	50	− 1.821e+003	− 2.29e+003	− 7.814e+001	− 1.382e+003	− 1.674e+003	− 3.06e+002	NA
	25	− 4.223+002	− 4.86e+002	− 1.68e+003	− 4.472e+003	− 1.57e+003	− 1.66e+003	NA
Beale	50	3.263e−016	2.31e−016	3.73e−016	7.61e−016	7.736e−016	3.42e−016	−
	25	4.265e−015	7.74e−015	1.135e−015	1.363e−017	7.56e−015	3.21e−015	−
Gold	50	3.00e+00	3.00e+00	3.00e+00	3.00e+00	3.00e+00	3.00e+00	NA
	25	3.00e+00	3.00e+00	3.00e+00	3.00e+00	3.00e+00	3.00e+00	NA
Schaffer N.4	50	3.053e−015	2.96e−001	2.921−001	2.934e−001	2.895e−001	2.791e−001	+
	25	2.921e−001	2.923e−001	2.924e−001	2.921e−001	2.923e−001	2.91e−991	NA
Michlewicz	50	− 7.642e+00	− 7.25e+00	− 7.45e+00	− 6.963e+00	− 6.851 e+00	− 1.231e+00	NA
	25	− 7.691e+00	− 7.69e+00	− 6.871e+00	− 7.351e+00	− 6.983e+00	− 6.453e+00	NA
Schaffer N.2	50	6.65e−016	8.881e−016	4.432e−016	6.556e−016	8.875e−016	4.141e−016	+
	25	1.334e−015	1.333e−015	6.664e−016	5.34e−015	1.334e−015	1.123e−015	−
Bird	50	− 1.0315e+002	− 1.069e+002	− 1.07e+002	− 1.067e+002	− 1.032e+002	− 1.06e+002	NA
	25	− 9.33e+001	− 1.045e+002	− 1.064e+002	− 1.044e+002	− 1.041e+002	− 1.05e+002	NA
HimmelBlau	50	1.65e−016	8.051e−016	3.831e−016	9.123e−016	1.461e−016	5.67e−016	−
	25	4.837e−015	4.42e−015	1.905e−015	3.951e−015	5.144e−015	2.13e−015	−
Booth	50	3.51e−016	2.061e−016	6.06e−016	7.078e−016	8.34e−016	3.075e−015	+
	25	1.81e−015	7.59e−016	1.93e−015	2.754e−015	6.471e−015	2.123e−015	−
Extended Cube	50	3.32e−015	4.981e−006	6.14e−008	1.936e−005	2.685e+00	2.182e−004	+
	25	5.71e−008	5.213e−005	7.103e−008	1.731e−005	2.921e+009	1.341e−005	+
Ackeley	50	7.18e−015	6.47e−012	7.96e−015	3.632e−013	3.093e+00	5.72e−009	+
	25	7.987e−015	5.021e−015	7.99e−015	3.593e−015	3.215e+00	3.123e−015	+
Rastrigin	50	1.795e+001	1.231e+002	7.49e+001	1.281e+002	1.52e+002	1.45e+001	NA
	25	3.65e+001	1.184e+002	8.171e+001	1.747e+002	1.672e+002	1.234e+001	NA
Griewank	50	9.987e−016	9.97e−016	1.65e−013	6.561e−013	1.075e+00	1.48e−008	+
	25	1.476e−002	9.215e−015	7.86e−015	5.074e−009	1.062e+00	1.47e−005	−
Rosenbrock	50	9.66e−016	1.073e−008	7.885e−016	3.97e−009	1.075e+005	5.81e−006	+
	25	3.981e+00	1.405e−008	6.94e−015	1.565e−011	7.151e+004	1.482e−011	−

Result: DiDE approach gives the best value for most of the benchmark functions. DiDE has higher mutation probability resulting in smaller CPU time. It also enhances exploration and avoids premature convergence

employing the supreme solution vector, this scheme improves earlier in contrast to the traditional schemes that uses only arbitrary vectors. The range of likely movement in the population escalates with enlarged pairs of solution and henceforth enhances the exploration of search space. This also aids to elude premature convergence and to avoid local minima. This procedure examines the division around each $X_{best,G}$, for every mutated point conserving the exploratory character and thereby improving the convergence. The donor vector attained from mutation strategy in Eq. (8) undergoes recombination to obtain the trial vector

using Eq. (6). Then thereafter, the variables enters into the selection process using Eq. (7).

4 Experimental settings of DiDE technique

DiDE technique was executed using MATLABr2017b and results were achieved along with the old-style mutation strategies. Five classical mutation approaches are taken along with proposed technique DiDE and outcomes were related. In the study performed, mutation constant F is assumed the value 0.6 and the crossover probability C_r is assumed the value 0.8. Fifteen varied functions were

Table 2 Test Statistics

Dimension	50
Chi square	23.8
df	5
Asymptotic Significance	0.0002

considered (for 50 and 25 dimensions) and the outcomes were computed by allotting the value to reach and the number of iterations.

Comparative study was performed on each of the above methods by fixing size and value-to-reach (VTR) for computing the best value, number of function evaluations and the CPU time of varied function methods. Table 1 shows the best value attained for dimension of 25 and 50. The table displays that for most of the benchmark function, the best value is obtained for the new variant DiDE. Certain function obtained virtuous outcomes for all types of classical DE strategies and DiDE algorithm. The total outcome gained demonstrates that DiDE technique is executed with improved efficiency in comparison to the classical DE method. The heightened results attained form DiDE technique is the resultant of using four varied control parameters. Friedman statistical test scores are steered on DiDE approach to authenticate the outcomes. On the basis of outcomes in Table 1, the Friedman statistical test was employed and consequences are tabularized in Table 2. Friedman test is applied on the data to check the global difference between the results attained using varied approaches. The asymptotic significance value in Table 2 shows that there is a significant difference between the different approaches tabulated in Table 1. The positions achieved after the Friedman statistical test are tabularized in Table 3. The ranks in Table 3 are obtained using the Bonferri Dunn procedure. This procedure is a post hoc test applied on Friedman Test to compare and rank the different approaches. The result in Table 3 shows that DiDE ranks second in terms of best value and ranks first when comparing the CPU time taken.

5 Fuzzy Tsallis entropy based multi-level thresholding on images

Thresholding is an elementary form of image separation where binary images are created from a gray scale image. Thresholding is generally done on a gray scale image. Color images can be threshold by designating distinct RGB components of the image. Thresholding procedures are of numerous types like histogram shape-based method, clustering based method, spatial method, local method and attribute-based method.

Based on the number of imagery sections, two kinds of thresholding are used: bi-level and multilevel. In bi-level thresholding, imagery is segmented in to two diverse sections. One section contains the pixels with gray value higher than a certain value 'T' while the second section occupies gray values smaller than 'T'. The initial section is identified as object pixels and the later as background pixels. In multi-level thresholding, the foreground and the background pixels are isolated into non-coinciding sets that assists in breaking the gray scale imagery into dissimilar units. Here, diverse values are allotted among dissimilar series of threshold points. Quantity of thresholds are specified beforehand.

Entropy is the numerical degree of randomness that can be used to illustrate the quality of input image. Entropy of an image with gray level between [0,m] is defined using Eq. (9) as:

$$\text{Entropy} = - \sum_0^m p_j * \log_2(p_j) \quad (9)$$

where, p_j is the probability that the difference between two adjoining pixels is equal to j and m is the gray level value. Low entropy has petite distinction among pixels and large course of pixels. High entropy has great dissimilarity among pixels. Let k be the value of threshold, μ_1 is the average value of all pixel entities between 0 and k , μ_2 is the average value of all pixel entities between $k + 1$ and 255, then the following condition should be satisfied.

$$k = \frac{\mu_1 + \mu_2}{2} \quad (10)$$

Table 3 Mean Ranking of various approaches

Strategy	Mean rank on best value	Mean rank on CPU time taken
DE/best/1	3.3	3.02
DE/best/2	3.7	3.1
DE/best-to-rand/1	2.5	2.3
DE/rand/1	3.22	2.5
DE/rand/2	5.01	4.5
DiDE	3.1	2.1

Let H_f and H_b be the entropy for foreground and background, then

$$H_f(T) = - \sum_{i=0}^k \frac{p(i)}{P_f(i)} * \log_2(\mu_f(i)) \tag{11}$$

$$H_b(T) = - \sum_{i=k+1}^{N-1} \frac{p(i)}{P_b(i)} * \log_2(\mu_b(i)) \tag{12}$$

where N is the overall quantity of pixels, $P_f(i)$ is the probability of foreground and $P_b(i)$ is the probability of background. μ is the degree of characteristics of image like brightness.

$$P_f(i) = \sum_{i=0}^k p(i) \tag{13}$$

$$P_b(i) = \sum_{i=k+1}^{N-1} p(i) \tag{14}$$

$$p(i) = \frac{h_i}{N} \tag{15}$$

where h_i is the quantity of pixels of gray level i . The optimal threshold value is selected by minimizing the entropy. This is depicted using Eq. (16).

$$T_{opt} = \operatorname{argmin} |H_f(T) - H_b(T)| \tag{16}$$

5.1 Applying DiDE strategy in fuzzy tsallis entropy based multi-level thresholding for Image Segmentation

In this work, an improved DiDE approach has been introduced to fuzzy tsallis entropy based thresholding. Fuzzy entropy based multilevel thresholding faces major drawback of high computational time and high complexity. So by combining fuzzy tsallis entropy based thresholding technique with high performance evolutionary approach like DE, we can improve the performance of image segmentation. As the new variant DiDE has enhanced performance in comparison to traditional DE approach, DiDE variant is embedded to fuzzy entropy technique to attain an accurate and faster computation. Initially, the input image is read and the number of thresholds is identified. Then the histogram value for the input image is calculated. Then the DiDE algorithm is applied on individual pixel values of the image where the pixel undergo mutation, crossover and selection to attain the ultimate resultant populace. The mutation strategy of DiDE is used as specified in Eq. (12). Fitness function for DiDE algorithm is given by the fuzzy entropy value using Eq. (9). Then selection and updating of the optimal entropy value is done if new entropy value is an improvement from the previous entropy values. The application of DiDE technique on pixel values is continued

until the termination condition is satisfied. Finally, the optimal entropy value attained using Eq. (16) is applied on the image and the segmented image will be obtained. The flowchart for the anticipated method is shown in Fig. 1.

6 Experimental results

Image segmentation is performed on weather radar images to identify regions of air pollution clearly. Using segmentation techniques, we can separately cluster the image according to the definite wavelength band. The anticipated DiDE approach was applied to the fuzzy Tsallis entropy technique to accomplish multi-level thresholding on image. Two illustrations of weather radar images were taken from www.temis.nl [30] for testing this technique. TEMIS is a web-based facility to acquire atmospheric satellite data. The satellite data consist mainly of satellite imagery showing tropospheric trace gasses, aerosol levels, changing composition of earth’s atmosphere, etc. that provides statistical information to climatologist. The satellite gadgets used for acquiring these datasets are mainly GOME, GOME-2, SCIAMACHY and OMI. These datasets are analyzed to provide sufficient information regarding air quality, air pollution level, UV radiations etc.

The samples of satellite imagery collected from TEMIS were segmented and analyzed. The new technique was compared with other image segmentation approaches like Shannon entropy, Kapur’s entropy and classical DE approach. Entropy of image and CPU time utilized is

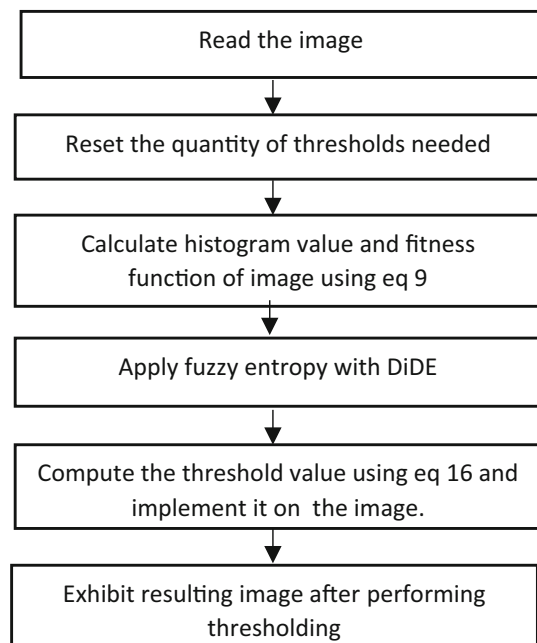
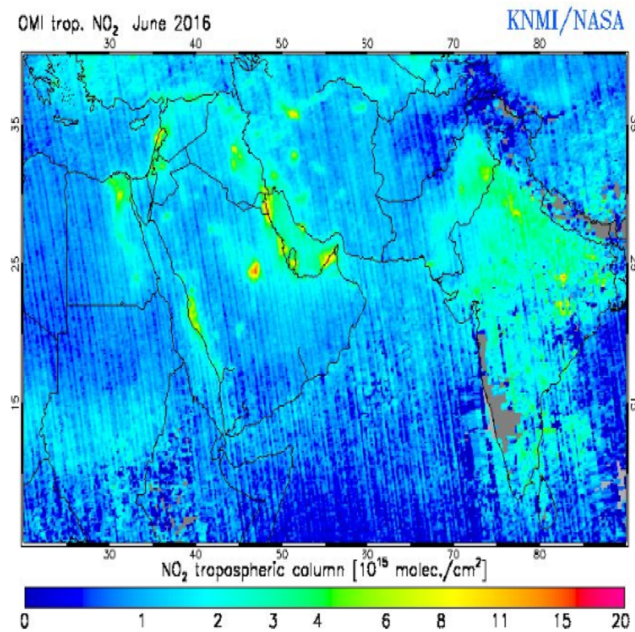
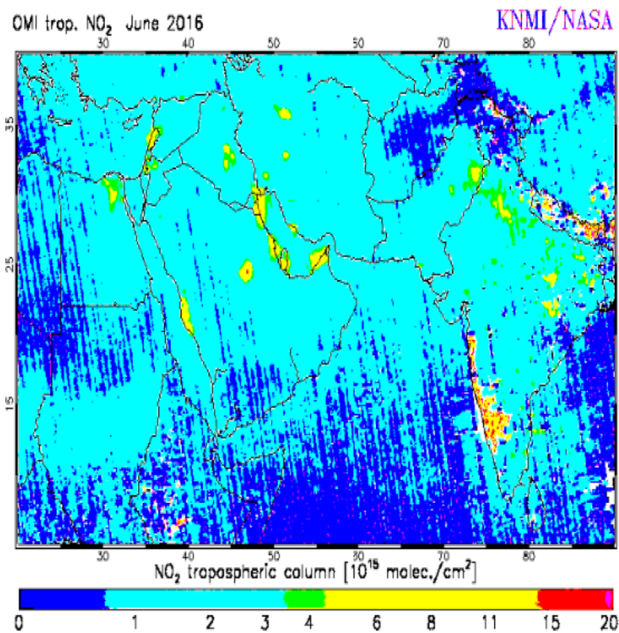


Fig. 1 Flowchart for multi-level thresholding with DiDE

Monthly mean tropospheric NO₂ from OMI for June 2016

Segmented image using DE algorithm



Segmented image using DiDE algorithm

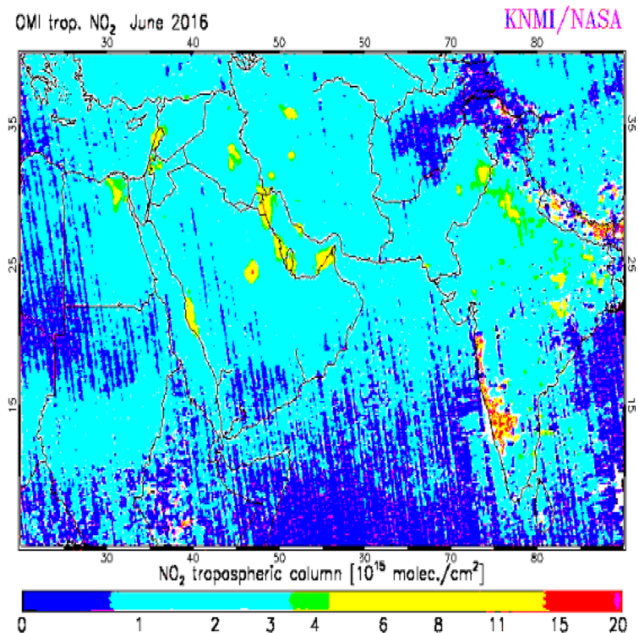


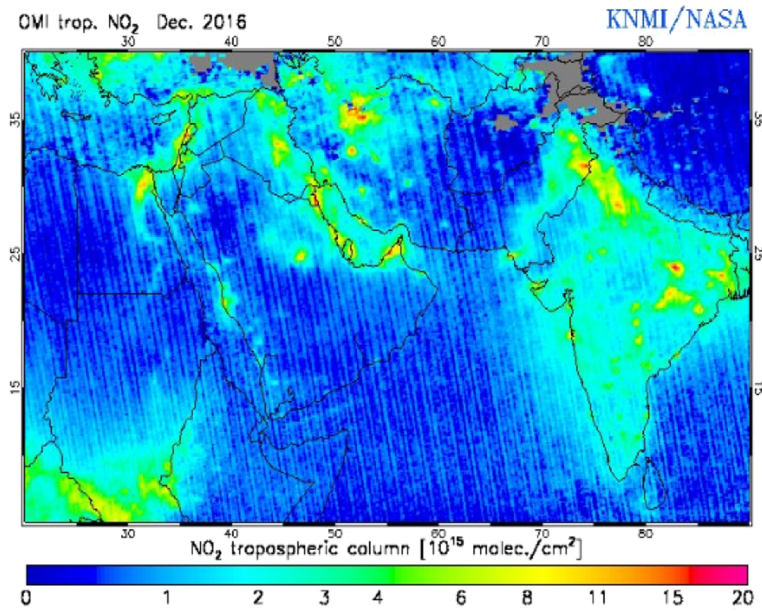
Fig. 2 Original imagery and segmented imagery using DE and DiDE

calculated and tabularized in Table. 4. The source picture and the picture after applying thresholding with DE and DiDE approach are displayed with Fuzzy tsallis entropy, Shannon entropy and Kapur's entropy in Figs. 2 and 3. The outcomes gained validates that DiDE approach gives

improved outcomes for multi-level thresholding in contrast to old-style DE approach.

The above tabulated values show that the result attained for DiDE approach-based thresholding is improved in comparison to the outcomes attained with DE approach. Two sample atmospheric remote sensory images of Air

Monthly mean tropospheric NO₂ from OMI for Dec 2016



Segmented image using DE algorithm

Segmented image using DiDE algorithm

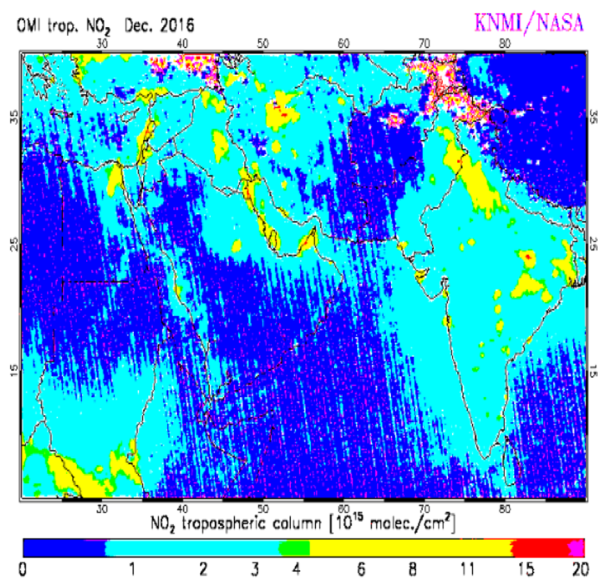
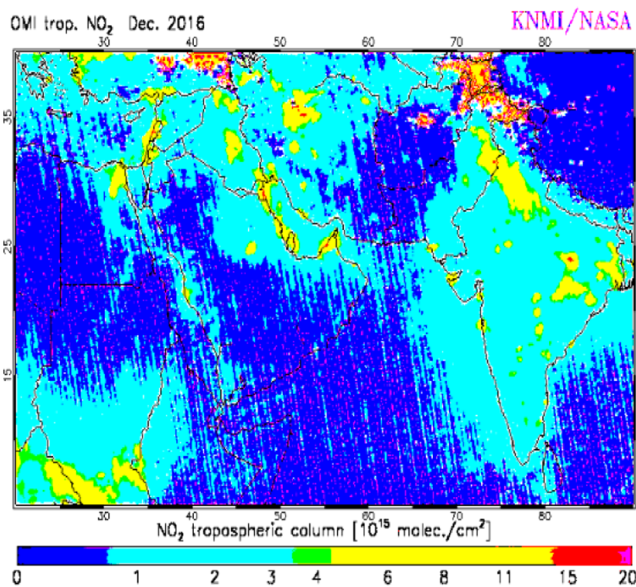


Fig. 3 Original image for Dec 2016 and segmented image using DE and DiDE

Pollution Monitoring: Nitrogen Dioxide (NO₂) are taken from [Temis 2017] and the multi-level thresholding is done on these images. The images after performing thresholding were separated on the basis of definite wavelength band. The images taken indicate the mean tropospheric NO₂ from OMI in the month of June and December of 2016. Figure 2 depicts the OMI in the month of June 2016 with the resultant segmented image using traditional DE and DiDE

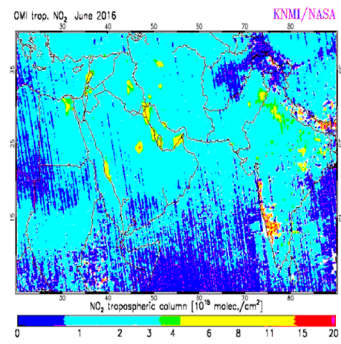
algorithm with Fuzzy Tsallis entropy technique and Fig. 3 depicts the OMI in the month of December 2016 with the resultant segmented image using traditional DE and DiDE algorithm with Fuzzy Tsallis entropy technique.

NO₂ is the result of oxidation of nitric oxide with the oxygen in air. It is emitted during combustion and burning of fuels. It belongs to a group of harmful gasses that depletes the atmosphere. It causes respiratory issues in

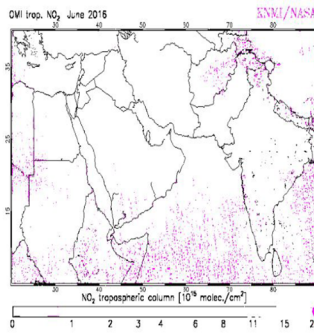
Fig. 4 Segmented image based on specific wavelength band

Monthly mean tropospheric NO₂ for June 2016

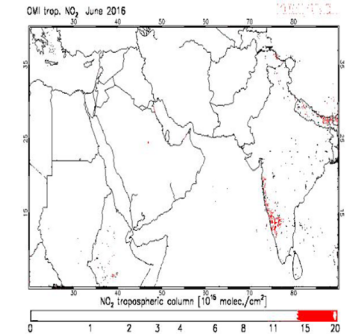
Threshold image using RDE



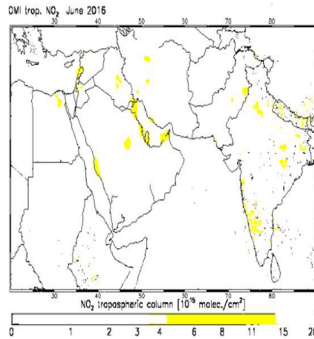
NO₂ tropospheric column greater than 20



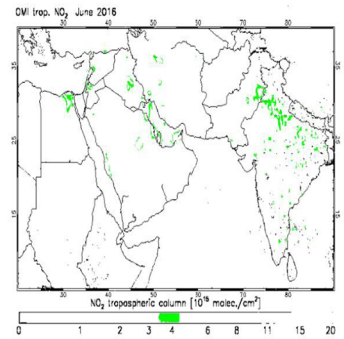
NO₂ tropospheric column between 15 ~ 20



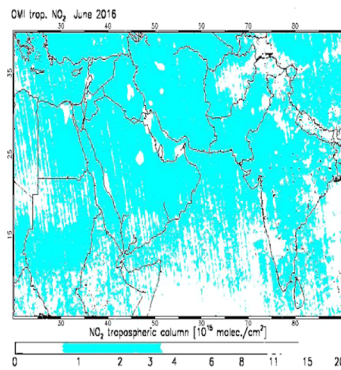
NO₂ tropospheric column between 4 ~ 15



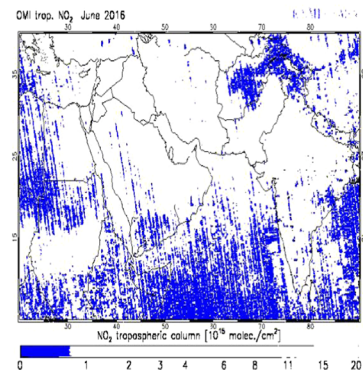
NO₂ tropospheric column between 3 ~ 4



NO₂ tropospheric column between 1 ~ 3



NO₂ tropospheric column between 0 ~ 1



NO₂ tropospheric column greater than 20 f
June 2016

NO₂ tropospheric column greater than 20 for
Dec 2016

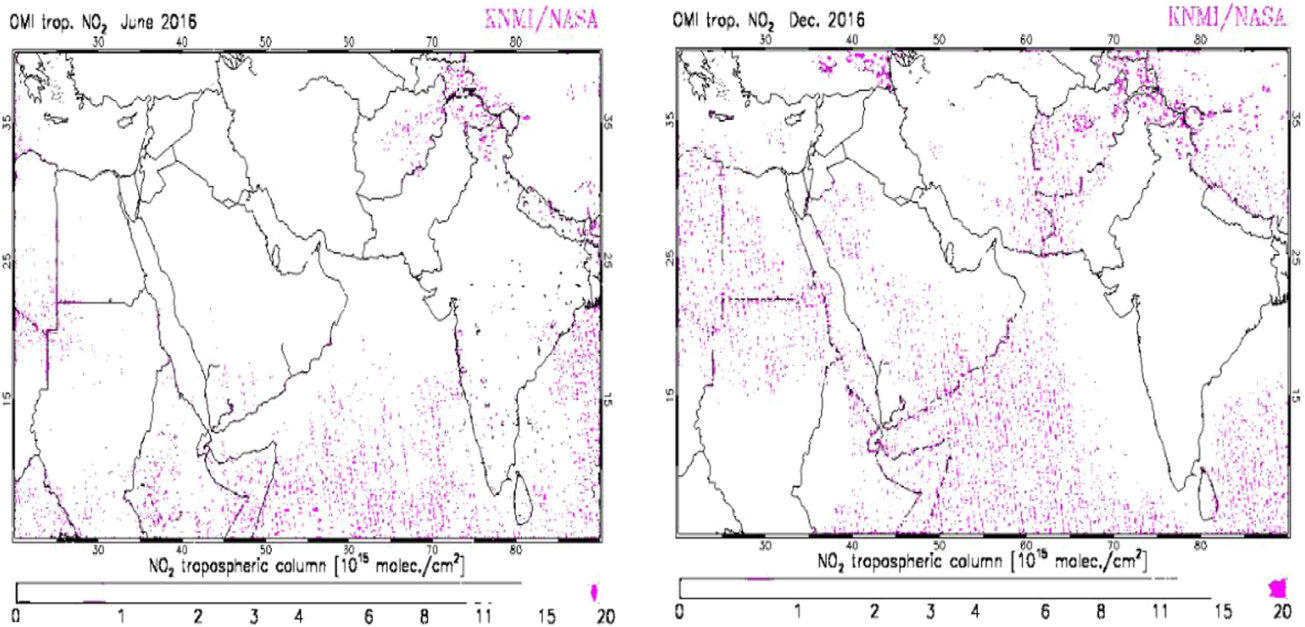


Fig. 5 Specific wavelength band for same region in June 2016 and Dec 2016

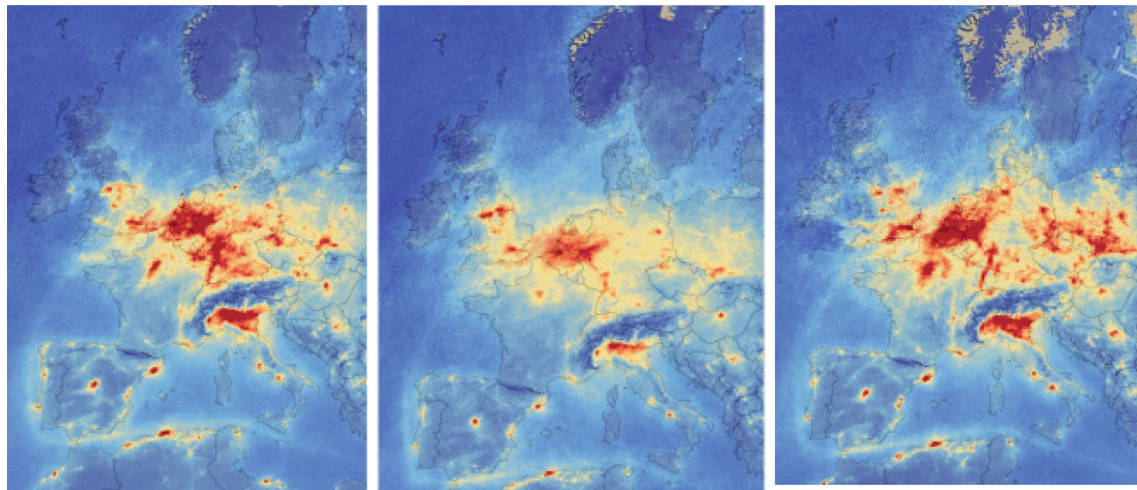


Fig. 6 Image of European region for March 2019, March 2020 and March 2021

human beings leading to asthma. So, by providing the clustered images according to wavelength, proper alerts can be given in regions of high emission of NO₂ and actions can be taken to reduce the level of NO₂. The clustered image according to the specific wavelength band is given in Fig. 3.

All scale in below figures are represented in measuring units 10¹⁵ mol/cm².

From Fig. 4, it is evident that the regions of high level of NO₂ can be easily detected. The separate clustered image

can be compared for various months to see the changes in the level of harmful gasses. Diverse colors on the image depict dissimilar wavelength band of NO₂ tropospheric column. The violet/pink color bar shows the wavelength band greater than 20 units. The red color bar shows the wavelength band between 15 and 20 units. The yellow color bar shows wavelength band between 4 and 15 units and the green color bar shows wavelength band between 3 ~ 4 units. Light blue color bar shows wavelength band between 1 and 3 units and dark blue color bar shows

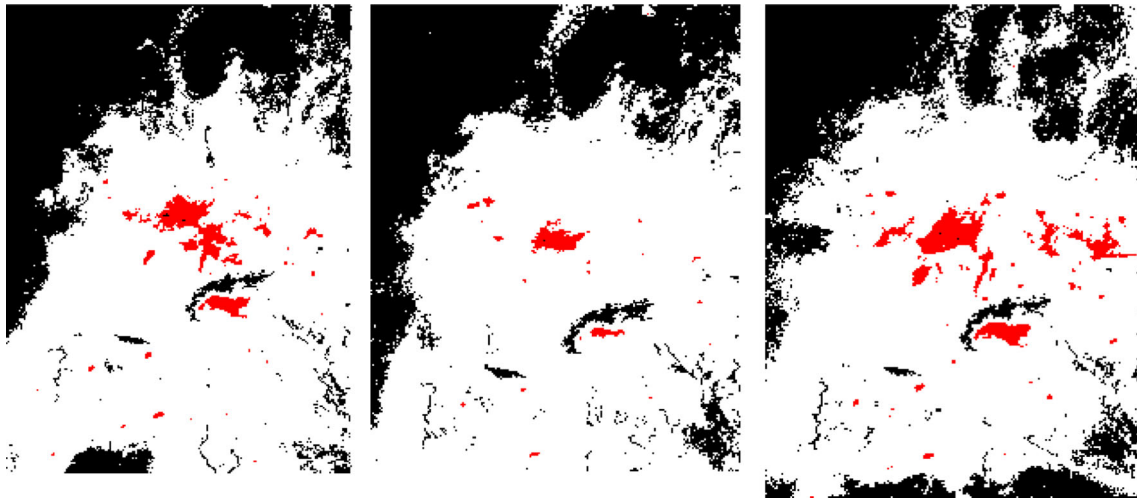


Fig. 7 Segmented image for high concentration of nitrogen dioxide

Table 4 Outcomes attained on image after applying thresholding

Image	Technique	Entropy	CPU time
Image 1	Thresholding built on Shannon Entropy	0.89	14.3
	Thresholding built on Kapur's entropy	0.91	15.1
	Thresholding built on fuzzy tsalli with DE	0.901	15.43
	Thresholding built with classical DE	0.92	14.43
	Thresholding built on fuzzy tsallis with DiDE	0.938	12.4
Image 2	Thresholding built on Shannon Entropy	0.903	15.1
	Thresholding built on Kapur's entropy	0.89	13.2
	Thresholding built on fuzzy tsallis with DE	0.91	14.03
	Thresholding built with classical DE	0.921	13.31
	Thresholding built on fuzzy tsallis with DiDE	0.94	11.21

wavelength band less than 1unit. After segmenting the images, the regions of high pollution can be easily identified. Figure 5 depicts the wavelength band greater than 20 units for the same region for the month of June 2016 and December 2016. Here, by comparing the two segmented images, we clearly identify the increase/decrease in air pollution in specific regions in the satellite imagery.

The segmented image helps in easily identifying whether the rate of pollution has increased or decreased for a specific region during the course of time. From the above resultant images, it is clearly seen that pollution of above 20 units has increased from June 2016 to December 2016. This observation helps in taking necessary actions to control the pollution rate and to avoid dangerous situations.

The segmented image of a particular region helps to study the change of air quality in the same region for a particular period of time. Figure 6 shows the imagery of the satellite image of European region for the period of March 2019, March 2020 and March 2021. The image displays the average concentration of NO_2 in air which was recorded using Copernicus Sentinel-5P satellite. By

viewing the original satellite imagery, it is challenging to easily identify regions of high pollution. By segmenting the imagery based on wavelength band of NO_2 concentration, we can easily get regions of high and low pollution. By comparing the segmented imagery for particular period of time, we can easily show the increase/ decrease in air pollution for the region. The above images were segmented according to its wavelength band using the proposed segmentation technique of multilevel thresholding using DiDE.

Figure 7 shows the segmented image for very high level of NO_2 for the wavelength band between 15 and 20 units. The segmented image clearly helps us to study the increase or decrease of NO_2 air pollution in a particular region and take action accordingly. For example, in the above segmented imagery, the NO_2 concentration above Brussels has decreased between March 2019 and March 2020. But by March 2021, the segmented imagery shows that the NO_2 concentration of the same region has risen to little more than the concentration in March 2019. Copernicus Sentinel missions provide open data of satellite imagery that helps

scientists to assess the air quality globally. Through the technique provided in the paper, we can easily segregate the regions based on different wavelength of NO_2 .

7 Conclusions

In the anticipated work, DiDE technique was introduced and the technique was tested using fifteen benchmark functions. The outcomes are compared to traditional mutation strategies of DE. DiDE was then applied to fuzzy Tsallis entropy based multi-level thresholding. The thresholding results were enhanced for DiDE approach in assessment to old-style DE method. The threshold image was further isolated on the basis of definite wavelength level. Presently the approach is implemented on atmospheric remote sensing imagery from TEMIS and Copernicus Sentinel-5P satellite. By using this technique, we can easily identify regions of high air pollution and take remedial actions accordingly. Also timely comparison of regions based on air pollutant can be easily performed for related studies. The quality of the resultant imagery is compared with segmented results using other techniques and the approach mentioned in this work is found to be of superior quality. This work can be done on similar remote sensing images from other projects or instruments like MOPITT, SCIAMACHY, GOME, etc.

Data availability The weather radar image dataset that support the findings of this study are available in TEMIS repository which is accessed through www.temis.nl/index.php link.

Declarations

Conflict of interest Authors affirm that there is no conflict of interest.

Reference:s

- Storn R, Price K (1997) Differential evolution—a simple and efficient heuristic for global optimization over continuous spaces. *J Glob Optim* 11(4):341–359
- Tang L, Tian L, Steward BL (2000) Color image segmentation with genetic algorithm for in-field weed sensing. *Trans ASAE-Am Soc Agric Eng* 43(4):1019–1028
- Tsai A, Anthony Y, Alan SW (2001) Curve evolution implementation of the Mumford-Shah functional for image segmentation, denoising, interpolation, and magnification. *IEEE Trans Image Process* 10(8):1169–1186
- Jiang T, Yang F (2002) An evolutionary tabu search for cell image segmentation. *IEEE Trans Syst Man Cybern Part B (Cybernetics)* 32(5):675–678
- Tao WB, Tian JW, Liu J (2003) Image segmentation by three-level thresholding based on maximum fuzzy entropy and genetic algorithm. *Pattern Recogn Lett* 24(16):3069–3078
- Ramos V, Fernando M (2004) Image colour segmentation by genetic algorithms. arXiv preprint cs/0412087
- Omran M, Engelbrecht AP, Salman A (2005) Particle swarm optimization method for image clustering. *Int J Pattern Recognit Artif Intell* 19(03):297–321
- Das S, Abraham A, Konar A (2006) Spatial information based image segmentation using a modified particle swarm optimization algorithm. In: *Intelligent systems design and applications, 2006. ISDA'06. Sixth International Conference on, vol 2. IEEE.* pp 438–444
- Omran MG, Salman A, Engelbrecht AP (2006) Dynamic clustering using particle swarm optimization with application in image segmentation. *Pattern Anal Appl* 8(4):332
- Talbi H, Mohamed B, Amer D (2007) A quantum-inspired evolutionary algorithm for multiobjective image segmentation. *Int J Math Phys Eng Sci* 1(2):109–114
- Maitra M, Chatterjee A (2008) A hybrid cooperative–comprehensive learning based PSO algorithm for image segmentation using multilevel thresholding. *Expert Syst Appl* 34(2):1341–1350
- Maulik U (2009) Medical image segmentation using genetic algorithms. *IEEE Trans Inf Technol Biomed* 13(2):166–173
- Das S, Sil S (2010) Kernel-induced fuzzy clustering of image pixels with an improved differential evolution algorithm. *Inf Sci* 180(8):1237–1256
- Ma M, Jianhui L, Min G, Fan Y, Yin Y (2011) SAR image segmentation based on Artificial Bee Colony algorithm. *Appl Soft Comput* 11(8):5205–5214
- Ghamisi P, Couceiro MS, Benediktsson JA, Nuno MFF (2012) An efficient method for segmentation of images based on fractional calculus and natural selection. *Expert Syst Appl* 39(16):12407–12417
- Sarkar S, Das S (2013) Multilevel image thresholding based on 2D histogram and maximum Tsallis entropy—a differential evolution approach. *IEEE Trans Image Process* 22(12):4788–4797
- Bhandari AK, Singh VK, Kumar A, Singh GK (2014) Cuckoo search algorithm and wind driven optimization based study of satellite image segmentation for multilevel thresholding using Kapur's entropy. *Expert Syst Appl* 41(7):3538–3560
- Sağ T, Çunkaş M (2015) Color image segmentation based on multiobjective artificial bee colony optimization. *Appl Soft Comput* 34:389–401
- Ramadas M, Abraham A, Kumar S (2016) ReDE—a revised mutation strategy for differential evolution algorithm. *Int J Intell Eng Syst* 9:51–58
- Meng Z, Pan JS (2016) QUasi-affine TRansformation Evolutionary (QUATRE) algorithm: a parameter-reduced differential evolution algorithm for optimization problems. In: *2016 IEEE congress on evolutionary computation (CEC), IEEE,* pp 4082–4089
- Suresh S, Lal S (2017) Modified differential evolution algorithm for contrast and brightness enhancement of satellite images. *Appl Soft Comput* 61:622–641
- Meng Z, Pan JS, Tseng KK (2019) PaDE: an enhanced Differential Evolution algorithm with novel control parameter adaptation schemes for numerical optimization. *Knowl-Based Syst* 168:80–99
- Meng Z, Pan JS (2019) HARD-DE: Hierarchical archive based mutation strategy with depth information of evolution for the enhancement of differential evolution on numerical optimization. *IEEE Access* 7:12832–12854
- Ramadas M, Abraham A, Kumar S (2019) FSDE-forced strategy differential evolution used for data clustering. *J King Saud Univ Comput Inf Sci* 31:52–61
- Ramadas M, Abraham A (2020) Detecting tumours by segmenting MRI images using transformed differential evolution

- algorithm with Kapur's thresholding. *Neural Comput Appl* 32(10):6139–6149
26. Krishna GJ, Ravi V (2021) High utility itemset mining using binary differential evolution: An application to customer segmentation. *Expert Syst Appl* 181:115122
 27. Singh P, Bose SS (2021) A quantum-clustering optimization method for COVID-19 CT scan image segmentation. *Expert Syst Appl* 185:11563
 28. Singh P, Bose SS (2021) Ambiguous D-means fusion clustering algorithm based on ambiguous set theory: special application in clustering of CT scan images of COVID-19. *Knowl-Based Syst* 231:107432
 29. Singh P (2021) A type-2 neutrosophic-entropy-fusion based multiple thresholding method for the brain tumor tissue structures segmentation. *Appl Soft Comput* 103:107119
 30. [Temis, 2017] www.temis.nl/index.php (accessed on October 08, 2017)

Publisher's Note Springer Nature remains neutral with regard to jurisdictional claims in published maps and institutional affiliations.

Springer Nature or its licensor (e.g. a society or other partner) holds exclusive rights to this article under a publishing agreement with the author(s) or other rightsholder(s); author self-archiving of the accepted manuscript version of this article is solely governed by the terms of such publishing agreement and applicable law.